

Facile synthesis and PET imaging of a novel potential heart acetylcholinesterase tracer *N*-[¹¹C]methyl-3-[[dimethylamino)carbonyloxy]-2-(2',2'-diphenylpropionoxymethyl)pyridinium

Ji-Quan Wang,^a Michael A. Miller,^a Bruce H. Mock,^a John C. Lopshire,^b William J. Groh,^b Douglas P. Zipes,^b Gary D. Hutchins^a and Qi-Huang Zheng^{a,*}

^aDepartment of Radiology, Indiana University School of Medicine, Indianapolis, IN 46202, USA

^bDepartment of Medicine, Krannert Institute of Cardiology, Indiana University School of Medicine, Indianapolis, IN 46202, USA

Received 15 June 2005; revised 5 July 2005; accepted 6 July 2005

Available online 19 August 2005

Abstract—A new AChE tracer *N*-[¹¹C]methyl-3-[[dimethylamino)carbonyloxy]-2-(2',2'-diphenylpropionoxymethyl)pyridinium ([¹¹C]MDDP, [¹¹C]1) has been synthesized in 40–65% radiochemical yield. Initial PET dynamic studies of [¹¹C]MDDP in rat heart showed rapid heart uptake and blood pool clearance to give high-quality heart images. Blocking studies of [¹¹C]MDDP with pretreatment drug neostigmine in rats found only minor reductions in rat heart [¹¹C]MDDP retention. The results suggest that [¹¹C]MDDP delineates the heart very clearly, and the uptakes of [¹¹C]MDDP in rat heart might be related to non-specific binding. © 2005 Elsevier Ltd. All rights reserved.

The function of acetylcholinesterase (AChE) is to terminate nerve impulse transmission by hydrolyzing the neurotransmitter acetylcholine. There is overwhelming consensus that acute exposure to organophosphorus (OP) agents inhibits AChE and that toxicity and lethality arise due to inhibition of AChE.¹ The protection against OP poisoning in current prophylactic and therapeutic regimens is a pretreatment regimen consisting of pyridostigmine, the reversible, covalent AChE inhibitor; the muscarinic receptor antagonist atropine (ATR); and the AChE reactivator pralidoxime chloride. Additional treatment with diazepam has proven advantageous in attempts to prevent convulsions. These regimens provide extensive protection against OP intoxication in animals. However, treatment might be considerably simplified if drugs that possessed multiple protective functions were used. To test this hypothesis, a group of pyridophen analogues, binary pyridostigmine-aprophen prodrugs with differential inhibition of AChE, butyrylcholinesterase (BChE), and muscarinic receptors,

were designed, synthesized, and evaluated as therapeutic drugs by Leader et al.² The results show that the compound *N*-methyl-3-[[dimethylamino)carbonyloxy]-2-(2',2'-diphenylpropionoxymethyl)pyridinium (MDDP) iodide inhibited AChE selectively over BChE, with a bimolecular rate constant similar to that of pyridostigmine. Our objective is to develop heart AChE tracers for biomedical imaging of cardiac neurotransmission using positron emission tomography (PET).³ Many positron labeled AChE inhibitors have been developed and evaluated for the in vivo mapping of AChE. Radiotracers with a low selectivity of AChE over BChE, as well as moderate binding properties to AChE, have led to non-specific binding in AChE enzyme over-expressed areas, such as brain and heart regions.⁴ It was expected that this problem could be overcome using radiolabeled pyridophen analogues with an excellent anti-AChE activity and a high selectivity of AChE over BChE. We have previously developed [¹¹C]neostigmine,⁵ [¹¹C]edrophonium, and their analogues⁶ as potential PET heart imaging agents for AChE. These compounds exhibited either high non-specific accumulation in myocardial tissue or poor myocardial uptake and were considered unsuitable for imaging the vagal system of the heart. As part of this project we turned our efforts toward the development of [¹¹C]pyridostigmine and its

Keywords: *N*-[¹¹C]methyl-3-[[dimethylamino)carbonyloxy]-2-(2',2'-diphenylpropionoxymethyl)pyridinium; Tracer; Synthesis; Positron emission tomography; Acetylcholinesterase; Heart.

*Corresponding author. Tel.: +1 317 278 4671; fax: +1 317 278 9711; e-mail: qzheng@iupui.edu

labeled analogues ($[^{11}\text{C}]para$ -pyridostigmine and $[^{11}\text{C}]ortho$ -pyridostigmine) (Fig. 1).⁷ In this ongoing study, we investigated whether N - $[^{11}\text{C}]methyl$ -3-[[dimethylamino]carbonyloxy]-2-(2',2'-diphenylpropionoxymethyl)pyridinium ($[^{11}\text{C}]MDDP$, $[^{11}\text{C}]1$) could be used to map heart AChE in vivo. As part of our efforts to evaluate novel potential heart imaging agents, we synthesized the tracer $[^{11}\text{C}]MDDP$ and performed initial PET imaging studies of the tracer $[^{11}\text{C}]MDDP$ in rat heart.

The synthetic approach for the tracer $[^{11}\text{C}]MDDP$ is shown in Scheme 1. The synthesis of precursor and reference standard was performed using a modification of the literature procedure.² The key intermediate, 2-hydroxymethyl-3-dimethylaminocarbonyloxy-pyridine (**3**), was isolated by column chromatography as the

major product in 31% chemical yield from the carbamylation of 3-hydroxy-2-hydroxymethylpyridine HCl (**2**) with dimethylcarbamy chloride. The other two products isolated from the reaction mixture were found to be the isomeric carbamate and the bis-carbamate. The acylation agent 2,2-diphenylpropionyl chloride (**5**) was prepared from 2,2-diphenylpropionic acid (**4**) with thionyl chloride in 96% yield. Acylation of **3** with **5** afforded the carbamyl-ester precursor 3-[[dimethylamino]carbonyloxy]-2-(2',2'-diphenylpropionoxymethyl)pyridine (**6**) in 51% yield. The tertiary pyridine **6** was methylated with methyl triflate to give the dimethylamino]carbonyloxy]-2-(2',2'-diphenylpropionoxymethyl)pyridinium triflate (**1**) in 97% yield. A simple technique solid-phase extraction (SPE)^{5–9} for convenient labeling and isolation of $[^{11}\text{C}$ -methyl]quaternary

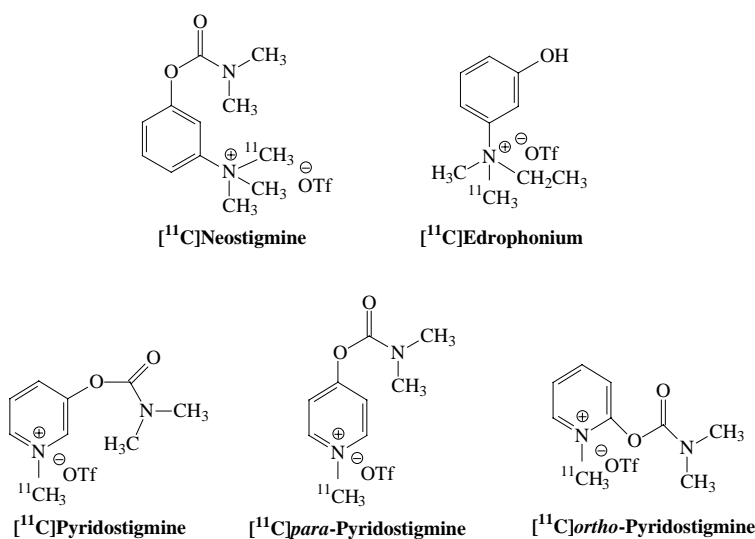
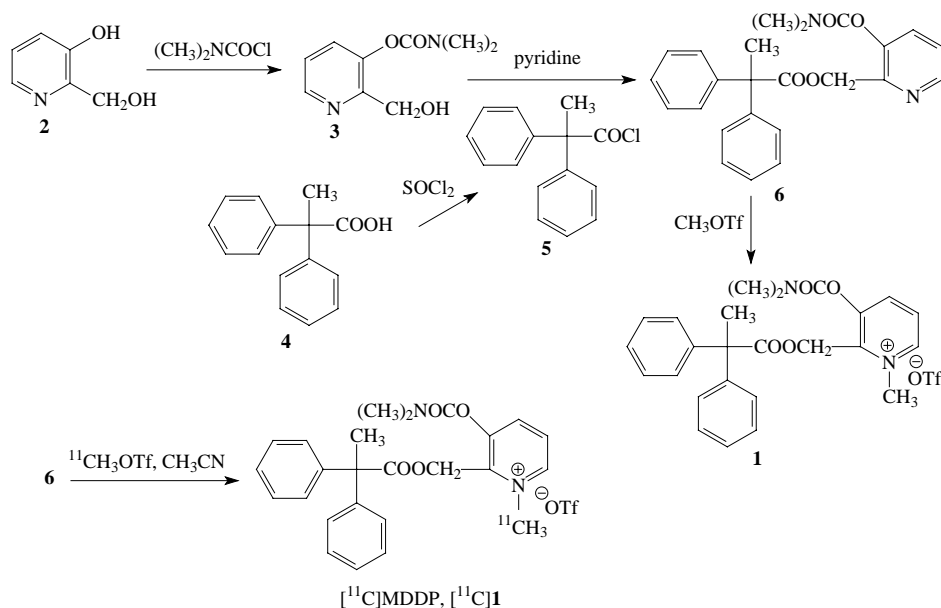


Figure 1. Chemical structures of $[^{11}\text{C}]neostigmine$, $[^{11}\text{C}]edrophonium$, $[^{11}\text{C}]pyridostigmine$, $[^{11}\text{C}]para$ -pyridostigmine, and $[^{11}\text{C}]ortho$ -pyridostigmine.



Scheme 1. Synthesis of N - $[^{11}\text{C}]methyl$ -3-[[dimethylamino]carbonyloxy]-2-(2',2'-diphenylpropionoxymethyl)pyridinium ($[^{11}\text{C}]MDDP$, $[^{11}\text{C}]1$).

amines by *N*-[^{11}C]methylation method was employed in the radiosynthesis of target tracer [^{11}C]MDDP ([^{11}C]1). The tertiary pyridine precursor **6** was labeled with [^{11}C]methyl triflate to provide quaternary pyridinium tracer [^{11}C]1 in 40–65% radiochemical yields, decay corrected to end of bombardment (EOB), and a synthesis time of 10–15 min. The key part in this technique is a SiO_2 Sep-Pak cartridge containing 0.5–2 g of adsorbent. It can be used to remove unreacted tertiary amine precursor **6**, reaction solvent acetonitrile, and unreacted [^{11}C]methyl triflate, which was decomposed by eluant ethanol. The final labeled product [^{11}C -methyl]quaternary amine [^{11}C]1 was eluted with an aqueous solution of 2% acetic acid, which can also contain up to 8% ethanol to enhance recovery of some [^{11}C -methyl]quaternary cations. The SPE technique was used for fast, efficient preparative separation of labeled product from its unlabeled precursor with large polarity difference, which shortened total synthesis and formulation time and afforded higher overall radiochemical yields. Chemical purity, radiochemical purity, and specific radioactivity were determined by the analytical HPLC method. The chemical purities of the precursor **6** and the reference standard **1** were >95%. The radiochemical purity of the target tracer [^{11}C]1 was >99%, and the chemical purity of the target tracer [^{11}C]1 was >93%. The specific radioactivity of the tracer [^{11}C]1 was 1.0–1.5 Ci/ μmol at end-of-synthesis (EOS).

In vivo dynamic PET imaging studies¹⁰ of the tracer [^{11}C]MDDP in young adult female Sprague–Dawley rats were performed in an IndyPET-II scanner^{11,12} for 60 min post iv injection of 0.2 mCi of the tracer in a rat, and the heart images in three rats are shown in the upper three panels in Figure 2. All PET images are coronal views. The image intensity is standard uptake value (SUV), averaged from 20 to 60 min after tracer injection. The color bar indicates approximate SUV for all three images. All PET images of the tracer [^{11}C]MDDP in rats 1, 2, and 3 showed that the heart was visible with the tracer. These images indicate that the new tracer delineates the heart very clearly. All images were acquired in list-mode and sorted into 15 \times 20 s frames, 10 \times 60 s frames, and 9 \times 300 s frames. Images were reconstructed using filtered back projection with a 70% Hanning filter (4.242 cm^{-1} cutoff frequency).

In vivo competitive inhibition studies were performed to assess the *in vivo* specificity of the tracer [^{11}C]MDDP to heart tissue AChE and whether the tracer distribution is susceptible to indirect pharmacological or pharmacodynamic effects that could complicate uptake site measurements. Competition or “blocking” study was carried out by pretreating groups of animals with drugs, unlabeled AChE inhibitors, which compete, or are believed to compete for the same binding site that the tracer interacts within the body. For the blocking imaging studies,¹⁰ the same three rats were pretreated by an intravenous injection of neostigmine prior to intravenous injection of the tracer [^{11}C]MDDP. The heart images in three rats are shown in the lower three panels in Figure 2. Likewise, all PET images are coronal views, the image inten-

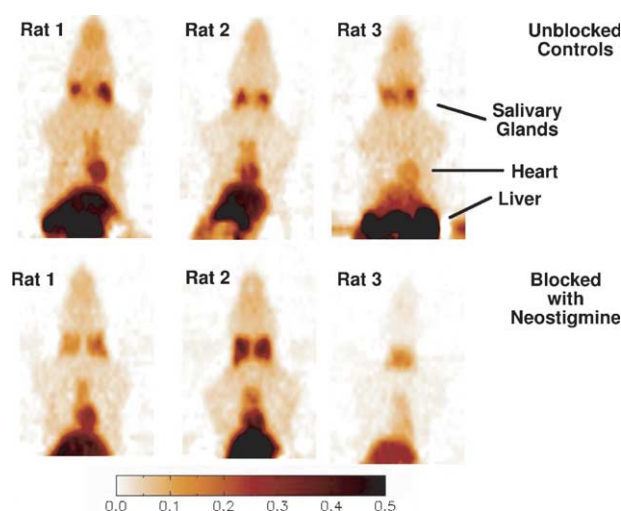


Figure 2. PET images of the tracer [^{11}C]MDDP in female rats anesthetized with acepromazine (0.2 mg/kg, im) and torbugesic (0.2 mg/kg, im), administered with 0.2 mCi radioactivity, and scanned with IndyPET-II for 60 min. The images are coronal slices from scans of three rats. The upper three panels show images after injection of [^{11}C]MDDP without a blocking agent. Image intensity is SUV averaged from 20 to 60 min after tracer injection. The lower three panels show images of the same three rats following administration of neostigmine as described in the text. The color bar indicates approximate SUV for all six images.

sity is SUV averaged from 20 to 60 min after tracer injection, and the color bar indicates approximate SUV for all three images. All PET images of the tracer [^{11}C]MDDP in rats 1, 2, and 3 showed that the heart was visible in blocking studies. A color scale normalizes all sets of data including unblocked control study and blocked with neostigmine study. Comparing the drug study with the control study, the partial blocking effect can be seen from the images.

The dynamic PET data of the tracer [^{11}C]MDDP with no blocker and with blocker neostigmine are shown in Figure 3. The plot Figure 3 is the individualized tracer heart uptake (*y*-axis) versus time from injection (*x*-axis), which indicated the kinetics of the tracer [^{11}C]MDDP with no blocker and with blocker neostigmine in three rats. The tracer uptake is expressed as the values, which are approximate SUV in the cardiac region of interest (ROI) plotted versus each time point in 60 min of entire scan time. The initial peak is the first pass of the tracer following the tail vein injection. The open symbols are values with no blocking agent in rats 1, 2, and 3 (control group). The filled symbols are values from scans, following the administration of the blocking agent neostigmine in the same three rats (blocking group). The tracer uptake was changed in the blocking study, which indicates a blocking drug effect on the binding of the radiotracer.

The mean and standard deviation (SD) SUV for heart ROIs of three rats in two different experimental groups (control group and blocking group) are given in Table 1, which shows the comparison of average tracer [^{11}C]MDDP uptake in the heart with no blocker and with blocker neostigmine in three rats. Likewise, Table 1 suggests that the partial blocking effect appeared in

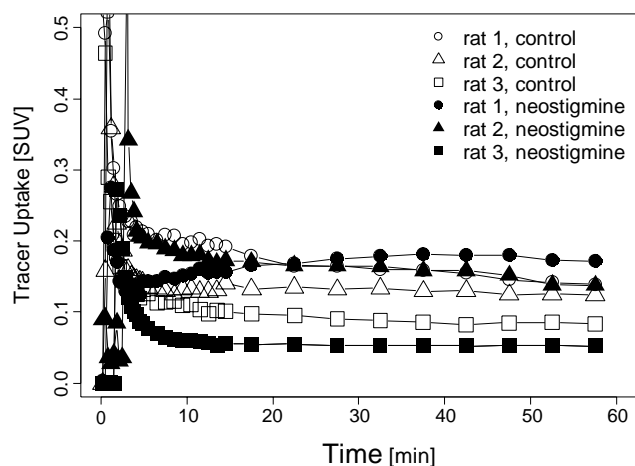


Figure 3. Kinetics of [^{11}C]MDDP in three rats. Values are approximate SUV in cardiac ROI plotted versus time from the beginning of scan. The initial peak is the first pass of the tracer, following the tail vein injection. The open symbols are values with no blocking agent. The filled symbols are values from scans, following the administration of neostigmine, as described in the text.

Table 1. Mean and standard deviation (SD) SUV for heart ROIs of three rats

Experimental group	Mean	SD
Control	0.125	0.034
Blocking with neostigmine	0.128	0.066
<i>p</i> value	0.87	

the blocking study. A *t* test comparing the means of the tracer [^{11}C]MDDP with no blocker and with blocker neostigmine gave a *p* value of 0.87, which did not denote the presence of a statistically significant difference. Initial PET blocking studies of the tracer [^{11}C]MDDP with pretreatment drug neostigmine in rats found only minor reductions in rat heart [^{11}C]MDDP retention. Therefore, we conclude there was no significant blocking in the data set and the uptakes of the tracer [^{11}C]MDDP in rat heart might be the results of non-specific binding. Based on the data available from the in vivo PET studies, we can assume that while in vitro experiments indicate efficacy of an AChE inhibitor MDDP iodide, kinetic factors, and rapid blood clearance make [^{11}C]MDDP unsuitable as tracers for PET imaging of AChE enzyme in the heart. This work demonstrates that the therapeutic drug and imaging tracer have different pharmacokinetic profiles. Further studies will determine whether the uptake site is AChE or if other binding sites are also involved.

Because of the high concentrations of AChE and BuChE in blood, as well as in heart and brain, it is extremely difficult to measure the blockade of cholinesterase function in these latter tissues. Typically, there is a narrow window between measurable blockade and lethality. In fact, it has been shown that blockade of blood AChE binding sites with neostigmine can increase the amount of AChE radiotracers available for binding in brain and likely heart as well. As 2 out of 3 of the rats used in this study actually exhibited increases in

[^{11}C]MDDP retention after administration of neostigmine, the possibility that what we describe as non-specific binding may actually be insufficient blockade of cholinesterase binding sites.

The experimental details are given for the new compound **1** and new tracer [^{11}C]1, and only characterization data are given for other known compounds **3**, **5**, and **6**.¹³ The experimental details for PET imaging studies are also given.¹⁴

In summary, the synthetic procedures that provide tertiary pyridine precursor **6**, quaternary pyridinium reference standard **1**, and quaternary pyridinium target tracer [^{11}C]1 have been well-developed. Initial PET dynamic studies of the tracer [^{11}C]1 in rat heart showed rapid heart uptake and blood pool clearance to give high-quality heart images. However, the results from the blocking studies of [^{11}C]MDDP with pretreatment drug neostigmine showed that no specific binding is present. These results suggest that the new tracer delineates the heart very clearly, the localization of [^{11}C]MDDP in rat heart might be mediated either by non-specific processes or by insufficient blockade of cholinesterase binding sites, and the visualization of [^{11}C]MDDP-PET on rat heart might be associated with non-specific binding or insufficient blockade of cholinesterase binding sites.

Acknowledgments

This work was partially supported by the Donald W. Reynolds Foundation and the Indiana Genomics Initiative (INGEN) of Indiana University, which is supported in part by Lilly Endowment Inc. The authors thank Winston Baity, Terry McBride, Tanya Martinez, and Kristan Boling for their assistance in animal studies. The referees' criticisms and editor's comments for the revision of the manuscript are greatly appreciated.

References and notes

- Duysen, E. G.; Li, B.; Xie, W.; Schopfer, L. M.; Anderson, R. S.; Broomfield, C. A.; Lockridge, O. J. *Pharmacol. Exp. Ther.* **2001**, *299*, 528.
- Leader, H.; Wolfe, A. D.; Chiang, P. K.; Gordon, R. K. *J. Med. Chem.* **2002**, *45*, 902.
- Carrio, I. J. *Nucl. Med.* **2001**, *42*, 1062.
- Ryu, E. K.; Choe, Y. S.; Park, E. Y.; Paik, J.-Y.; Kim, Y. R.; Lee, K.-H.; Choi, Y.; Kim, S. E.; Kim, B.-T. *Nucl. Med. Biol.* **2005**, *32*, 185.
- Mulholland, G. K.; Zheng, Q.-H.; Mock, B. H.; Carlson, K. A.; Giger, S.; Vavrek, M. T.; Fain, R. L.; Hutchins, G. D. *J. Nucl. Med.* **1999**, *40*(Suppl. 5), 495.
- Zheng, Q.-H.; Liu, X.; Fei, X.; Wang, J.-Q.; Mock, B. H.; Glick-Wilson, B. E.; Sullivan, M. L.; Hutchins, G. D. *Bioorg. Med. Chem. Lett.* **2003**, *13*, 1787.
- Wang, J.-Q.; Miller, M. A.; Fei, X.; Stone, K. L.; Lopshire, J. C.; Groh, W. J.; Zipes, D. P.; Hutchins, G. D.; Zheng, Q.-H. *Nucl. Med. Biol.* **2004**, *31*, 957.
- Mulholland, K. M.; Zheng, Q.-H.; Mock, B. H.; Vavrek, M. T. *J. Labelled Cpd. Radiopharm.* **1999**, *42*(Suppl. 1), S459.

9. Zheng, Q.-H.; Stone, K. L.; Mock, B. H.; Miller, K. D.; Fei, X.; Liu, X.; Wang, J.-Q.; Glick-Wilson, B. E.; Sledge, G. W.; Hutchins, G. D. *Nucl. Med. Biol.* **2002**, *29*, 803.
10. Zheng, Q.-H.; Fei, X.; DeGrado, T. R.; Wang, J.-Q.; Stone, K. L.; Martinez, T. D.; Gay, D. J.; Baity, W. L.; Mock, B. H.; Glick-Wilson, B. E.; Sullivan, M. L.; Miller, K. D.; Sledge, G. W.; Hutchins, G. D. *Nucl. Med. Biol.* **2003**, *30*, 753.
11. Rouze, N. C.; Hutchins, G. D. *IEEE Trans. Nucl. Sci.* **2003**, *50*, 1491.
12. Frese, T.; Rouze, N. C.; Bouman, C. A.; Sauer, K.; Hutchins, G. D. *IEEE Trans. Med. Imaging* **2003**, *22*, 258.
13. Experimental details and characterization data. (a) General: All commercial reagents and solvents were used without further purification unless otherwise specified. Melting points were determined with a MEL-TEMP II capillary tube apparatus and were uncorrected. ^1H NMR spectra were recorded on a Bruker QE 300 NMR spectrometer using tetramethylsilane (TMS) as an internal standard. Chemical shift data for the proton resonances were reported in parts per million (δ), relative to the internal standard TMS (δ 0.0). Low-resolution mass spectra (LRMS) were obtained using a Bruker Biflex III MALDI-ToF mass spectrometer, and high-resolution mass spectra (HRMS) were obtained using a Kratos MS80 mass spectrometer, in the Department of Chemistry at Indiana University. Chromatographic solvent proportions are expressed on a volume: volume basis. Thin layer chromatography was run using Analtech silica gel GF uniplates ($5 \times 10 \text{ cm}^2$). Plates were visualized by UV light. Normal phase flash chromatography was carried out on EM Science silica gel 60 (230–400 mesh) with a forced flow of the indicated solvent system in the proportions described below. All moisture-sensitive reactions were performed under a positive pressure of nitrogen maintained by a direct line from a nitrogen source. Analytical HPLC was performed using a Prodigy (Phenomenex) $5 \mu\text{m}$ C-18 column, $4.6 \times 250 \text{ mm}$; 3:1:1 $\text{CH}_3\text{CN}/\text{MeOH}/20 \text{ mM}$, pH 6.7 KHPO_4^- (buffer solution) mobile phase; flow rate 1.5 mL/min; and UV (240 nm) and γ -ray (NaI) flow detectors. Semi-prep SiO_2 Sep-Pak type cartridge was obtained from Waters Corporate Headquarters, Milford, MA. Sterile Millex-GS 0.22 μm vented filter unit was obtained from Millipore Corporation, Bedford, MA. (b) Compound **3**: a white solid, yield 31%, $R_f = 0.13$ (50:1 $\text{CH}_2\text{Cl}_2/\text{MeOH}$). ^1H NMR (CDCl_3 , 300 MHz) δ 8.42 (d, 1H, $J = 3.7 \text{ Hz}$, ring-H), 7.55 (dd, 1H, $J_1 = 8.1 \text{ Hz}$, $J_2 = 1.5 \text{ Hz}$, ring-H), 7.27 (dd, 1H, $J_1 = 8.1 \text{ Hz}$, $J_2 = 5.1 \text{ Hz}$, ring-H), 4.73 (s, 2H, CH_2OH), 4.22 (br s, 1H, OH), 3.13 (s, 3H, CH_3), 3.03 (s, 3H, CH_3). (c) Compound **5**: a white solid, yield 96%, mp 35–37 °C. ^1H NMR (CDCl_3 , 300 MHz) δ 7.18–7.42 (m, 10H, phenyl H), 2.09 (s, 3H, CH_3). (d) Compound **6**: a colorless oil, yield 51%, $R_f = 0.48$ (1:1 EtOAc/hexane). ^1H NMR (CDCl_3 , 300 MHz) δ 8.42 (dd, 1H, $J_1 = 4.4 \text{ Hz}$, $J_2 = 1.5 \text{ Hz}$, pyridyl H), 7.56 (dd, 1H, $J_1 = 8.1 \text{ Hz}$, $J_2 = 1.5 \text{ Hz}$, pyridyl H), 7.30 (dd, 1H, $J_1 = 8.1 \text{ Hz}$, $J_2 = 5.2 \text{ Hz}$, pyridyl H), 7.18–7.25 (m, 10H, phenyl H), 5.31 (s, 2H, CH_2), 2.94 (s, 3H, CH_3N), 2.87 (s, 3H, CH_3N), 1.92 (s, 3H, CH_3). (e) Compound **1**: Methyl triflate (115 μL , 1.016 mmol) was added to a solution of compound **6** (0.41 g, 1.014 mmol) in dry CH_2Cl_2 (10 mL) at room temperature. The solution was stirred for 30 min. TLC showed no starting material left. The solvent was removed under vacuum to give compound **1** (0.56 g, 97%) as a white solid, mp 43–45 °C. ^1H NMR (CDCl_3 , 300 MHz) δ 8.64 (d, 1H, $J = 6.6 \text{ Hz}$, pyridyl H), 8.34 (d, 1H, $J = 8.8 \text{ Hz}$, pyridyl H), 7.90 (dd, 1H, $J_1 = 8.9 \text{ Hz}$, $J_2 = 5.9 \text{ Hz}$, pyridyl H), 7.02–7.30 (m, 10H, phenyl H), 5.58 (s, 2H, CH_2), 4.08 (s, 3H, N^+CH_3), 3.11 (s, 3H, NCH_3), 3.01 (s, 3H, NCH_3), 1.90 (s, 3H, CH_3). LRMS (EI, m/z): 181 (100%), 419 [(M-OTf) $^+$, 1.8%]. HRMS (EI, m/z): calcd for $\text{C}_{25}\text{H}_{27}\text{O}_4\text{N}_2$: 419.1970, found: 419.1971. (f) Tracer [^{11}C]**1**: The precursor (**6**, 0.5 mg) was dissolved in acetonitrile (250 μL). The mixture was transferred to a small volume, three-necked reaction tube. [^{11}C]Methyl triflate was passed into an air-cooled reaction tube at a temperature between -15 and -20 °C, which was generated by a Venturi cooling device powered with 100 psi compressed air, until radioactivity in solution reached a maximum (2–3 min), and then the reaction tube was isolated and heated at 70–80 °C for 2–3 min. The reaction tube was connected to the Silica Sep-Pak. The labeled product solution mixture was passed onto the SiO_2 Sep-Pak for SPE purification by gas pressure. The reaction tube and Sep-Pak were washed with ethanol (5 mL), and the washing solution was discarded to a waste bottle. The final product [^{11}C]**1** was eluted from the Sep-Pak with 90:8:2 $\text{H}_2\text{O}/\text{EtOH}/\text{HOAc}$ (2–4 mL), sterile-filtered through a 0.22 μm cellulose acetate membrane, and collected into a sterile vial. The pH was adjusted to 5.5–7.0 with 2 M NaOH and 150 mM NaH_2PO_4 mixed solution (1/20, 0.2–0.4 mL). Total radioactivity was assayed and the total volume (2.5–5.0 mL) was noted. The overall synthesis time was 10–15 min. The decay corrected yields, from $^{11}\text{CO}_2$, were 40–65%, and the radiochemical purity was >99% by analytical HPLC. Retention times in the analytical HPLC system were: RT₆ = 4.51 min, RT[^{11}C]**1** = 2.83 min. The chemical purity of the target tracer was >93%.
14. (a) Dynamic IndyPET-II imaging of the tracer [^{11}C]MDDP in the rats. All animal experiments were performed under a protocol approved by the Indiana University Institutional Animal Care and Use Committee. The female Sprague-Dawley rat (250–300 g) was anesthetized with acepromazine (0.2 mg/kg, im) and torbugesic (0.2 mg/kg, im). 0.2 mCi of [^{11}C]MDDP was administered intravenously to the rat via the tail vein. The micro-PET images of the tracer were acquired in IndyPET-II scanner by the ordered subset expectation maximization (OSEM) using 6 subsets/4 iterations for 60 min dynamic scans from a rat post intravenous injection of 0.2 mCi of the tracer, and frame durations were defined as 300 s for entire 3600 s scan. (b) Blocking IndyPET-II imaging of the tracer [^{11}C]MDDP in the rats with pretreatment drug neostigmine. For the blocking experiments, the rats (250–300 g) were pretreated by an intravenous injection in the tail vein with 3.0 mg/kg of neostigmine in saline 30 min, prior to iv injection of 0.2 mCi [^{11}C]MDDP in the tail vein. After tracer administration, the animals were handled, as described above. (c) Statistical analysis. Differences between neostigmine pretreated group and control group were examined for statistical significance using Student's *t* test. A *p* value less than 0.05 denoted the presence of a statistically significant difference.